Recent advances in 3D full-waveform inversion (FWI) for site characterization

Challenges and open issues

Loukas F. Kallivokas

Mechanics, Uncertainty, and Simulation in Engineering
Department of Civil, Architectural, and Environmental Engineering

and

The Institute for Computational Engineering and Sciences

The University of Texas at Austin

MUSE
THE UNIVERSITY OF TEXAS AT AUSTIN · COCKRELL SCHOOL OF ENGINEERING
DEPARTMENT OF CIVIL, ARCHITECTURAL AND ENVIRONMENTAL ENGINEERING
MECHANICS, UNCERTAINTY, AND SIMULATION IN ENGINEERING

Outline

Site characterization (SC) by full-waveform inversion (FWI)

Overarching goal: to reconstruct the material profile of probed, semi-infinite, near-surface, geologic formations using elastic waves for interrogation, and surface records of the complete waveforms of the formation's response in the time-domain

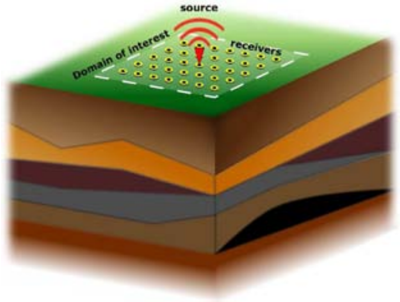

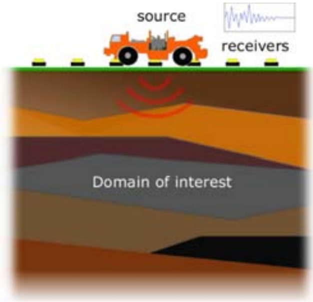

SC by FWI - The framework and its challenges

- An imaging problem: infer properties from sensor data
- Sensor deployment is limited - setting inferior to medical imaging
- Properties are spatially distributed
- No *a priori* simplifying assumptions (geometry; layering; etc)
- Physics drives discretization $\rightarrow$ millions of unknown properties; for a 100m$\times$100m$\times$20m domain: 2 million elastic properties
- SC focuses on near-surface deposits: domain truncation needed
- Exploration geophysics drives advances
- Scale issues, complex physics, algorithmic challenges, open problem even for the acoustic case

SC by FWI - Recent advances in our work

Key problem ingredients:

- The forward problem
  - Resolve wave motion in unbounded, arbitrarily heterogeneous, domains
- FWI: an inverse medium problem
  - To address the imaging/inversion: PDE-constrained optimization framework
  - To address the scale: parallel computing
  - To address robustness: physics-based algorithmic tweaks

Outline

Perfectly-Matched-Layer (PML) truncated domains

Forward wave simulation problem - key characteristics

- Probed domain is arbitrarily heterogeneous
- Probed domain is semi-infinite in extent
- The ROI is rather limited in extent...need for domain truncation

Quality domain truncation is paramount $\longrightarrow$ PMLs

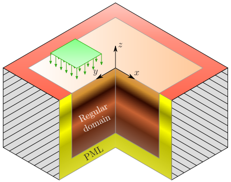

The PML is an absorbing condition

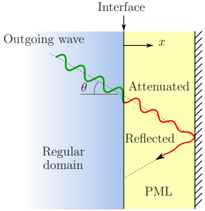

The concept

The PML is a buffer zone that surrounds a truncated finite computational domain. Within the buffer, the propagating waves are forced to decay exponentially, without generating reflections from the interface (perfectly matched).

Advantages

- **absorbs** waves without reflection for **all non-zero** angles-of-incidence and frequencies
- can handle arbitrary heterogeneity
- has tunable parameters

Hybrid formulation (optimal)

Standard displacement-based elastodynamics for Ω^{RD}
Mixed-field (stress-displacement) formulation for Ω^{PML}

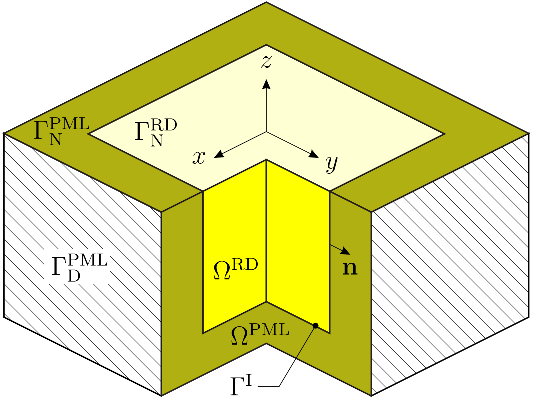

The IBVP (3rd-order in time)

Find $\mathbf{u}(\mathbf{x},t) \in \Omega^{\mathrm{RD}} \cup \Omega^{\mathrm{PML}}$, $\mathbf{S}(\mathbf{x},t) \in \Omega^{\mathrm{PML}}$, such that:

$$\mathbf{div}\left\{\mu\left[\nabla\dot{\mathbf{u}} + (\nabla\dot{\mathbf{u}})^T\right] + \lambda(\operatorname{div}\dot{\mathbf{u}})\mathcal{I}\right\} + \dot{\mathbf{b}} = \rho\dddot{\mathbf{u}} \qquad \text{in } \Omega^{\mathrm{RD}} \times \mathrm{J}$$

$$\mathbf{div}\left(\ddot{\mathbf{S}}^T\Lambda_e + \dot{\mathbf{S}}^T\Lambda_p + \mathbf{S}^T\Lambda_w\right) = \rho\left(a\dddot{\mathbf{u}} + b\ddot{\mathbf{u}} + c\dot{\mathbf{u}} + d\mathbf{u}\right) \qquad \text{in } \Omega^{\mathrm{PML}} \times \mathrm{J}$$

$$\begin{aligned} a\dddot{\mathbf{S}} + b\ddot{\mathbf{S}} + c\dot{\mathbf{S}} + d\mathbf{S} &= \mu\left[(\nabla\ddot{\mathbf{u}})\Lambda_e + \Lambda_e(\nabla\ddot{\mathbf{u}})^T + (\nabla\dot{\mathbf{u}})\Lambda_p + \Lambda_p(\nabla\dot{\mathbf{u}})^T\right] \\ &+ \mu\left[(\nabla\mathbf{u})\Lambda_w + \Lambda_w(\nabla\mathbf{u})^T\right] + \lambda\left[\operatorname{div}(\Lambda_e\ddot{\mathbf{u}}) + \operatorname{div}(\Lambda_p\dot{\mathbf{u}}) + \operatorname{div}(\Lambda_w\mathbf{u})\right]\mathcal{I} \qquad \text{in } \Omega^{\mathrm{PML}} \times \mathrm{J} \end{aligned}$$

BCs:

$$\left\{\mu\left[\nabla\dot{\mathbf{u}} + (\nabla\dot{\mathbf{u}})^T\right] + \lambda(\operatorname{div}\dot{\mathbf{u}})\mathcal{I}\right\}\mathbf{n}^+ = \dot{\boldsymbol{g}}_n \qquad \text{on } \Gamma_{\mathrm{N}}^{\mathrm{RD}} \times \mathrm{J}$$

$$(\ddot{\mathbf{S}}^T\Lambda_e + \dot{\mathbf{S}}^T\Lambda_p + \mathbf{S}^T\Lambda_w)\mathbf{n}^- = \mathbf{0} \qquad \text{on } \Gamma_{\mathrm{N}}^{\mathrm{PML}} \times \mathrm{J}$$

$$\mathbf{u} = \mathbf{0} \qquad \text{on } \Gamma_{\mathrm{D}}^{\mathrm{PML}} \times \mathrm{J}$$

$$\mathbf{u}^+ = \mathbf{u}^- \qquad \text{on } \Gamma^{\mathrm{I}} \times \mathrm{J}$$

$$\left\{\mu\left[\nabla\dot{\mathbf{u}} + (\nabla\dot{\mathbf{u}})^T\right] + \lambda(\operatorname{div}\dot{\mathbf{u}})\mathcal{I}\right\}\mathbf{n}^+ + (\ddot{\mathbf{S}}^T\Lambda_e + \dot{\mathbf{S}}^T\Lambda_p + \mathbf{S}^T\Lambda_w)\mathbf{n}^- = 0 \qquad \text{on } \Gamma^{\mathrm{I}} \times \mathrm{J}$$

Semi-discrete form

$$\mathbf{M}\dddot{\mathbf{d}} + \mathbf{C}\ddot{\mathbf{d}} + \mathbf{K}\dot{\mathbf{d}} + \mathbf{G}\mathbf{d} = \dot{\mathbf{f}}$$

$$\textit{or}\ \mathbf{M}\ddot{\mathbf{d}} + \mathbf{C}\dot{\mathbf{d}} + \mathbf{K}\mathbf{d} + \mathbf{G}\bar{\mathbf{d}} = \mathbf{f}, \qquad \bar{\mathbf{d}} = \int_0^t \mathbf{d}(\tau)|_{\mathrm{PML}}\, d\tau \quad \Rightarrow \quad \dot{\bar{\mathbf{d}}} = \mathbf{d}|_{\mathrm{PML}}$$

$$\mathbf{M} = \begin{bmatrix} \bar{\mathbf{M}}_{\mathrm{RD}} + \bar{\mathbf{M}}_a & \mathbf{0} \\ \mathbf{0} & \mathbf{N}_a \end{bmatrix} \qquad \mathbf{C} = \begin{bmatrix} \bar{\mathbf{M}}_b & \bar{\mathbf{A}}_{eu} \\ -\bar{\mathbf{A}}_{el}^T & \mathbf{N}_b \end{bmatrix} \qquad \mathbf{K} = \begin{bmatrix} \bar{\mathbf{K}}_{\mathrm{RD}} + \bar{\mathbf{M}}_c & \bar{\mathbf{A}}_{pu} \\ -\bar{\mathbf{A}}_{pl}^T & \mathbf{N}_c \end{bmatrix}$$

$$\mathbf{G} = \begin{bmatrix} \bar{\mathbf{M}}_d & \bar{\mathbf{A}}_{wu} \\ -\bar{\mathbf{A}}_{wl}^T & \mathbf{N}_d \end{bmatrix} \qquad \mathbf{d} = \begin{bmatrix} \mathbf{u}_h & \mathbf{S}_h \end{bmatrix}^T \qquad \mathbf{f} = \begin{bmatrix} \bar{\mathbf{f}}_{\mathrm{RD}} & \mathbf{0} \end{bmatrix}^T$$

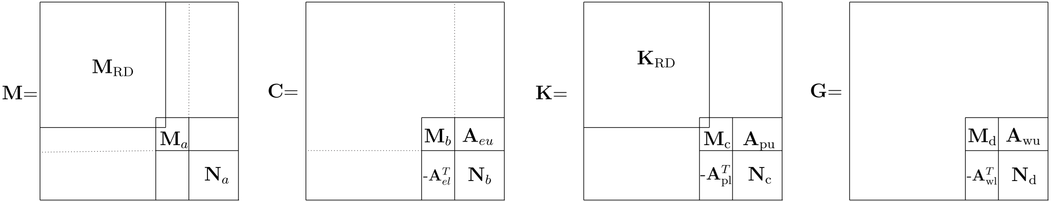

Temporal discretization

Temporal integration:

$$\mathbf{M}\ddot{\mathbf{d}} + \mathbf{C}\dot{\mathbf{d}} + \mathbf{K}\mathbf{d} + \mathbf{G}\bar{\mathbf{d}} = \mathbf{f}, \qquad \bar{\mathbf{d}} = \int_0^t \mathbf{d}(\tau)|_{\mathrm{PML}}\, d\tau \quad \Rightarrow \quad \dot{\bar{\mathbf{d}}} = \mathbf{d}|_{\mathrm{PML}}$$

A couple of choices $\rightarrow$ implicit Newmark Method

$$\begin{bmatrix} \mathbf{M} & \mathbf{0} \\ \mathbf{0} & \mathbf{0} \end{bmatrix} \begin{bmatrix} \ddot{\mathbf{d}} \\ \ddot{\bar{\mathbf{d}}} \end{bmatrix} + \begin{bmatrix} \mathbf{C} & \mathbf{0} \\ \mathbf{0} & \mathbf{I} \end{bmatrix} \begin{bmatrix} \dot{\mathbf{d}} \\ \dot{\bar{\mathbf{d}}} \end{bmatrix} + \begin{bmatrix} \mathbf{K} & \mathbf{G} \\ -\mathbf{I} & \mathbf{0} \end{bmatrix} \begin{bmatrix} \mathbf{d} \\ \bar{\mathbf{d}} \end{bmatrix} = \begin{bmatrix} \mathbf{f} \\ \mathbf{0} \end{bmatrix}$$

Un-Symmetric 1

$$\begin{bmatrix} \mathbf{M} & \mathbf{0} \\ \mathbf{0} & \mathbf{I} \end{bmatrix} \begin{bmatrix} \ddot{\mathbf{d}} \\ \ddot{\bar{\mathbf{d}}} \end{bmatrix} + \begin{bmatrix} \mathbf{C} & \mathbf{0} \\ -\mathbf{I} & \mathbf{0} \end{bmatrix} \begin{bmatrix} \dot{\mathbf{d}} \\ \dot{\bar{\mathbf{d}}} \end{bmatrix} + \begin{bmatrix} \mathbf{K} & \mathbf{G} \\ \mathbf{0} & \mathbf{0} \end{bmatrix} \begin{bmatrix} \mathbf{d} \\ \bar{\mathbf{d}} \end{bmatrix} = \begin{bmatrix} \mathbf{f} \\ \mathbf{0} \end{bmatrix}$$

Un-Symmetric 2

A better choice using spectral elements $\rightarrow$ explicit Runge-Kutta method

$$\frac{d}{dt} \begin{bmatrix} \mathbf{x}_0 \\ \mathbf{x}_1 \\ \mathbf{M}\mathbf{x}_2 \end{bmatrix} = \begin{bmatrix} \mathbf{0} & \mathbf{I} & \mathbf{0} \\ \mathbf{0} & \mathbf{0} & \mathbf{I} \\ -\mathbf{G} & -\mathbf{K} & -\mathbf{C} \end{bmatrix} \begin{bmatrix} \mathbf{x}_0 \\ \mathbf{x}_1 \\ \mathbf{x}_2 \end{bmatrix} + \begin{bmatrix} \mathbf{0} \\ \mathbf{0} \\ \mathbf{f} \end{bmatrix}$$

where $\mathbf{x}_0 = \bar{\mathbf{d}},\ \mathbf{x}_1 = \mathbf{d},\ \mathbf{x}_2 = \dot{\mathbf{d}}$.

Numerical experiment: heterogeneous medium with inclusion

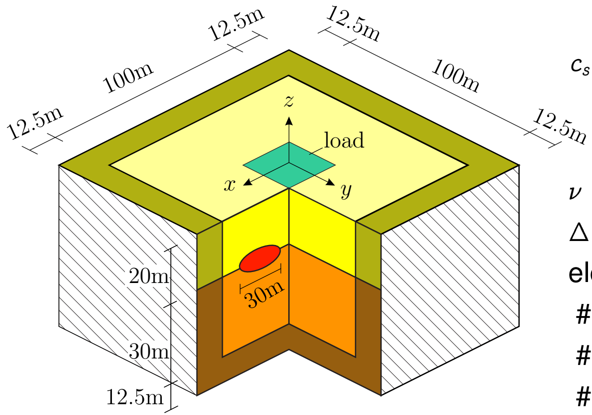

$$c_s(z) = \begin{cases} 400 \text{ m/s}, & -20m \leq z \leq 0m \\ 500 \text{ m/s}, & -50m \leq z < -20m \\ 600 \text{ m/s}, & \text{ellipsoidal inclusion} \end{cases}$$

$\nu = 0.25$

$\Delta t = 4.8 \times 10^{-4} s$

element size $= 1.25m$

\# elements $= 500'000$

\# unknowns $= 24'228'426$

\# unknowns ED $= 521'884'704$

PML parameters:

$m = 2$

$\alpha_o = 5$

$\beta_o = 500$

Displacements time histories

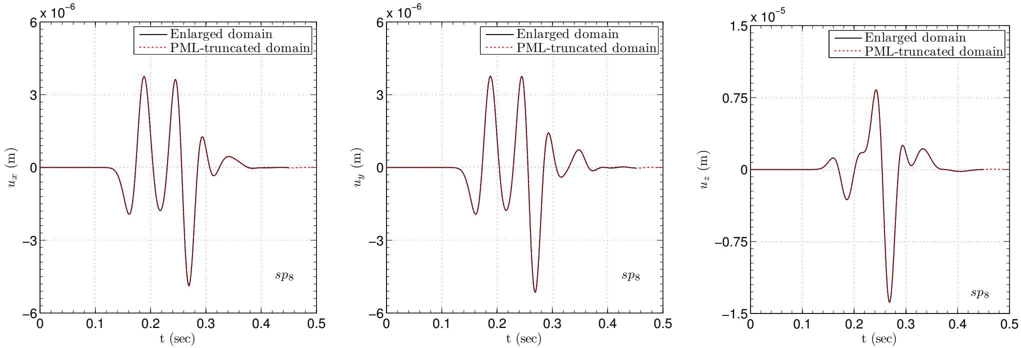

Energy decay

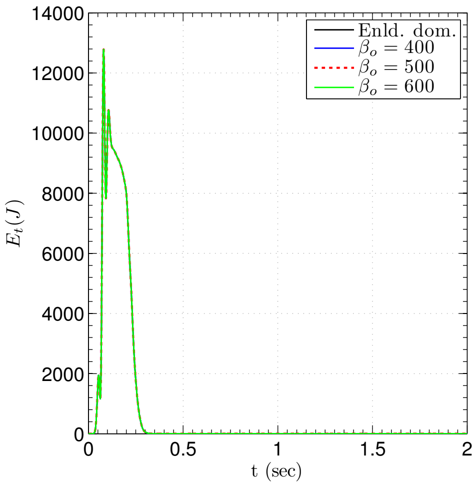

standard scale

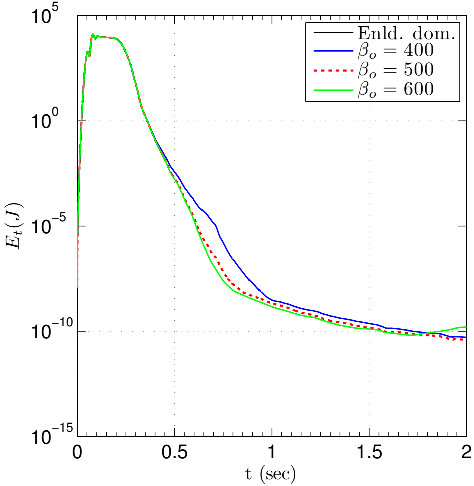

logarithmic scale

Long-time stability

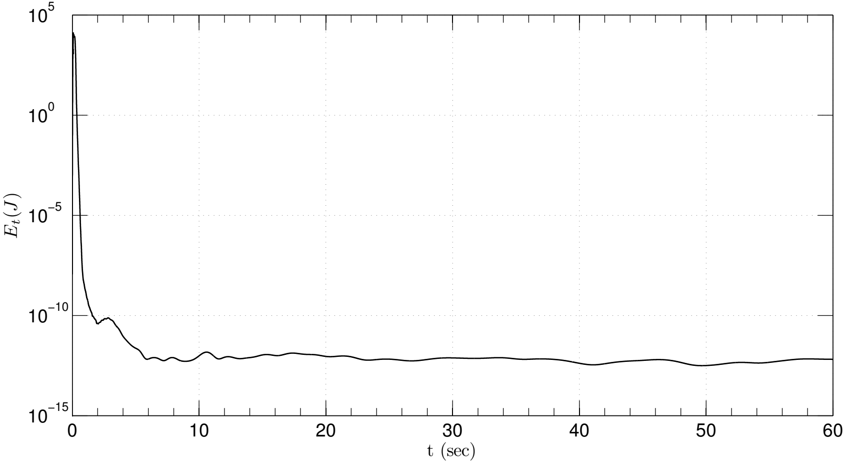

125'000 time steps ($\beta_o = 500$)

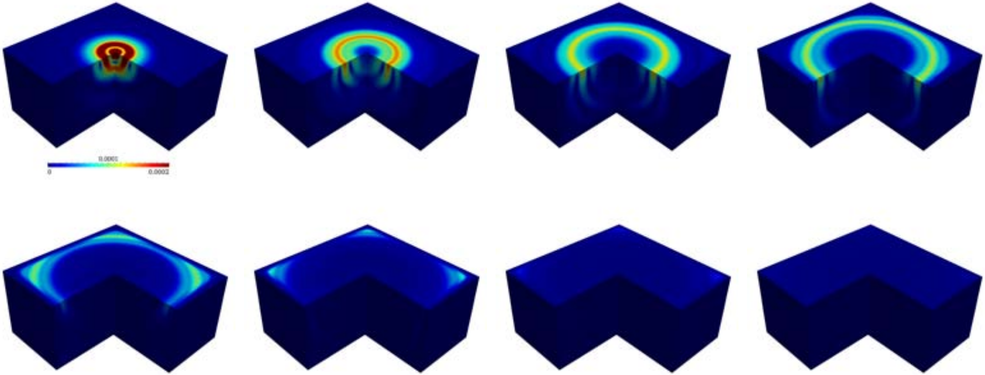

Snapshots of total displacement taken at $t = 0.111, 0.147, 0.183, 0.219, 0.255, 0.291, 0.327, 0.363$ s.

PML accuracy - relative error

Error at sampling points between hybrid-PML and enlarged domain solutions

sample point	x	y	z	error (Example 1)	error (Example 2)
sp1	0	0	0	1.17×10^{-12}	4.61×10^{-10}
sp2	+50	0	0	2.52×10^{-8}	6.07×10^{-7}
sp3	+50	0	-25	2.89×10^{-9}	2.87×10^{-6}
sp4	+50	0	-50	1.46×10^{-7}	7.03×10^{-6}
sp5	0	0	-50	9.86×10^{-9}	1.41×10^{-5}
sp6	+50	+50	0	3.26×10^{-7}	1.86×10^{-6}
sp7	+50	+50	-25	5.50×10^{-8}	6.72×10^{-6}
sp8	+50	+50	-50	5.08×10^{-7}	6.44×10^{-6}

Outline

Goal: find the distribution of material properties $\lambda(x), \mu(x)$

PDE-constrained optimization problem:

$$\min_{\lambda,\mu} \mathcal{J}(\lambda,\mu) := \overbrace{\frac{1}{2}\sum_{j=1}^{N_r}\int_0^T\int_{\Gamma_m}(\mathbf{u}-\mathbf{u}_m)\cdot(\mathbf{u}-\mathbf{u}_m)\,\delta(\mathbf{x}-\mathbf{x}_j)\,\mathrm{d}\Gamma\; dt}^{\text{data misfit}} + \overbrace{\mathcal{R}(\lambda,\mu)}^{\text{regularization}}$$

`subject to the continuous forward problem`

Regularization:

$$\mathcal{R}^{TN}(\lambda,\mu) = \frac{R_\lambda}{2}\int_\Omega \nabla\lambda\cdot\nabla\lambda\; d\Omega + \frac{R_\mu}{2}\int_\Omega \nabla\mu\cdot\nabla\mu\; d\Omega$$

$$\mathcal{R}^{TV}(\lambda,\mu) = \frac{R_\lambda}{2}\int_{\Omega^{\mathrm{RD}}}(\nabla\lambda\cdot\nabla\lambda+\epsilon)^{\frac{1}{2}}\,\mathrm{d}\Omega + \frac{R_\mu}{2}\int_{\Omega^{\mathrm{RD}}}(\nabla\mu\cdot\nabla\mu+\epsilon)^{\frac{1}{2}}\,\mathrm{d}\Omega$$

The Lagrangian functional

$$
\begin{aligned}
\mathcal{L}(\mathbf{u},\mathbf{S},\mathbf{w},\mathbf{T},\lambda,\mu) := {} & \frac{1}{2}\sum_{j=1}^{N_r}\int_0^T\int_{\Gamma_m}(\mathbf{u}-\mathbf{u}_m)\cdot(\mathbf{u}-\mathbf{u}_m)\,\delta(\mathbf{x}-\mathbf{x}_j)\,\mathrm{d}\Gamma\,dt + \mathcal{R}(\lambda,\mu) \\
& - \int_0^T\int_{\Omega^{\mathrm{RD}}}\nabla\mathbf{w}:\left\{\mu\left[\nabla\mathbf{u}+(\nabla\mathbf{u})^T\right]+\lambda(\operatorname{div}\mathbf{u})\mathcal{I}\right\}\,\mathrm{d}\Omega\,dt \\
& - \int_0^T\int_{\Omega^{\mathrm{PML}}}\nabla\mathbf{w}:\left(\dot{\mathbf{S}}^T\Lambda_e+\mathbf{S}^T\Lambda_p+\bar{\mathbf{S}}^T\Lambda_w\right)\,\mathrm{d}\Omega\,dt - \int_0^T\int_{\Omega^{\mathrm{RD}}}\mathbf{w}\cdot\rho\ddot{\mathbf{u}}\,\mathrm{d}\Omega\,dt \\
& - \int_0^T\int_{\Omega^{\mathrm{PML}}}\mathbf{w}\cdot\rho\,(a\ddot{\mathbf{u}}+b\dot{\mathbf{u}}+c\mathbf{u}+d\bar{\mathbf{u}})\,\mathrm{d}\Omega\,dt + \int_0^T\int_{\Gamma_{\mathrm{N}}^{\mathrm{RD}}}\mathbf{w}\cdot\boldsymbol{g}_n\,\mathrm{d}\Gamma\,dt \\
& + \int_0^T\int_{\Omega^{\mathrm{RD}}}\mathbf{w}\cdot\mathbf{b}\,\mathrm{d}\Omega\,dt - \int_0^T\int_{\Omega^{\mathrm{PML}}}\mathbf{T}:\left(a\ddot{\mathbf{S}}+b\dot{\mathbf{S}}+c\mathbf{S}+d\bar{\mathbf{S}}\right)\,\mathrm{d}\Omega\,dt \\
& + \int_0^T\int_{\Omega^{\mathrm{PML}}}\mathbf{T}:\mu\left[(\nabla\dot{\mathbf{u}})\Lambda_e+\Lambda_e(\nabla\dot{\mathbf{u}})^T+(\nabla\mathbf{u})\Lambda_p+\Lambda_p(\nabla\mathbf{u})^T+(\nabla\bar{\mathbf{u}})\Lambda_w+\Lambda_w(\nabla\bar{\mathbf{u}})^T\right] \\
& + \mathbf{T}:\lambda\left[\operatorname{div}(\Lambda_e\dot{\mathbf{u}})+\operatorname{div}(\Lambda_p\mathbf{u})+\operatorname{div}(\Lambda_w\bar{\mathbf{u}})\right]\mathcal{I}\,\mathrm{d}\Omega\,dt
\end{aligned}
$$

Optimality system

Stationarity enforced by the vanishing of first-order Gâteau derivatives

State (forward) problem: $\mathcal{L}'(\mathbf{u}, \mathbf{S}, \mathbf{w}, \mathbf{T}, \lambda, \mu)(\tilde{\mathbf{w}}, \tilde{\mathbf{T}}) = 0$

an initial value BVP

Adjoint problem: $\mathcal{L}'(\mathbf{u}, \mathbf{S}, \mathbf{w}, \mathbf{T}, \lambda, \mu)(\tilde{\mathbf{u}}, \tilde{\mathbf{S}}) = 0$

a final value BVP

Control problem:

$$\mathcal{L}'(\mathbf{u}, \mathbf{S}, \mathbf{w}, \mathbf{T}, \lambda, \mu)(\tilde{\lambda}) = 0$$

$$\mathcal{L}'(\mathbf{u}, \mathbf{S}, \mathbf{w}, \mathbf{T}, \lambda, \mu)(\tilde{\mu}) = 0$$

Algorithmic tweak: regularization factor continuation

$$\tilde{\mathbf{M}}\mathbf{g} = R\ \mathbf{g}_{\text{reg}} + \mathbf{g}_{\text{mis}}$$

Concept: "size" of $R\ \mathbf{g}_{\text{reg}}$ should be proportional to that of $\mathbf{g}_{\text{mis}}$

$$\mathbf{n}_{\text{reg}} = \frac{\mathbf{g}_{\text{reg}}}{||\mathbf{g}_{\text{reg}}||}, \qquad \mathbf{n}_{\text{mis}} = \frac{\mathbf{g}_{\text{mis}}}{||\mathbf{g}_{\text{mis}}||}$$

$$\tilde{\mathbf{M}}\mathbf{g} = ||\mathbf{g}_{\text{mis}}||\ \left(\wp\ \mathbf{n}_{\text{reg}} + \mathbf{n}_{\text{mis}}\right), \qquad \wp = R\,\frac{||\mathbf{g}_{\text{reg}}||}{||\mathbf{g}_{\text{mis}}||} \approx 0.5 \rightarrow 0.3$$

$$R = \wp\,\frac{||\mathbf{g}_{\text{mis}}||}{||\mathbf{g}_{\text{reg}}||}$$

Outline

Numerical Experiments

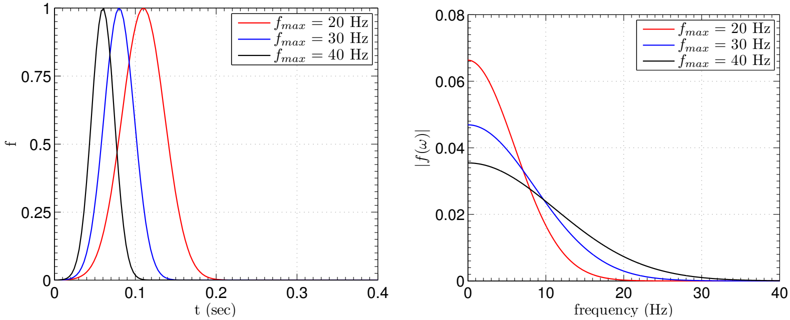

Example 1: smoothly-varying heterogeneous medium

Example 2: layered medium

Example 3: layered medium with inclusion

Example 4: layered medium with 3 inclusions

Example 1: setup

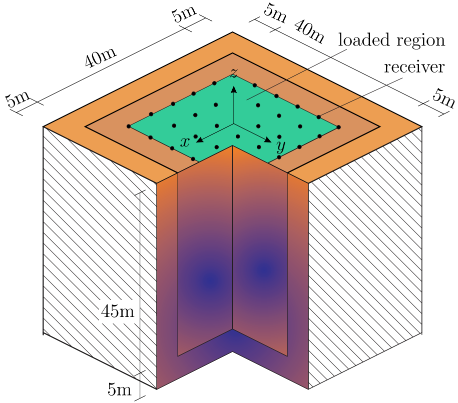

$$\lambda(z) = \mu(z) = 80 + 0.45\,|z| + 35\,\exp\left(-\frac{(|z|-22.5)^2}{150}\right)\ \text{(MPa)}$$

min $c_s = 200m/s$

max $c_p = 433m/s$

element size $= 1.25m$

$\Delta t = 10^{-3}s$

time steps $= 400/450$

elements $= 72'324$

state unknowns $= 3'578'136$

material unknowns $= 616'850$

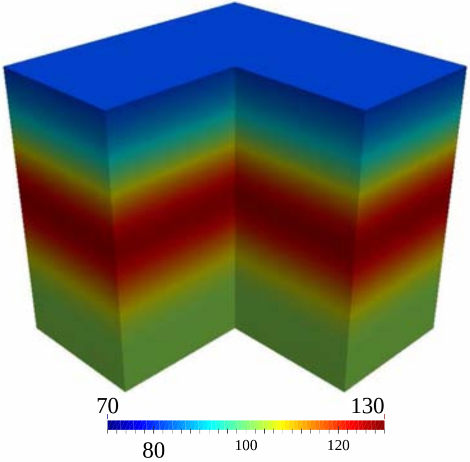

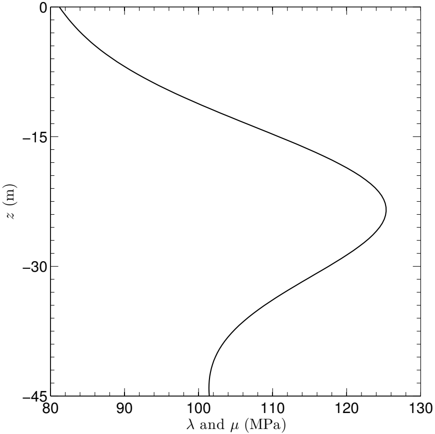

Smoothly varying medium: target λ and μ (MPa); and profile at $(x, y) = (0, 0)$

Single-parameter inversion (μ only)

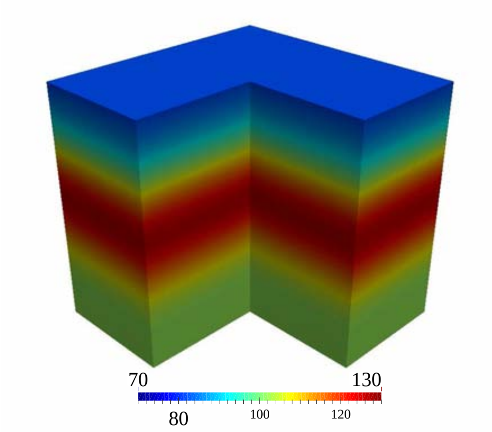

λ (a priori known)

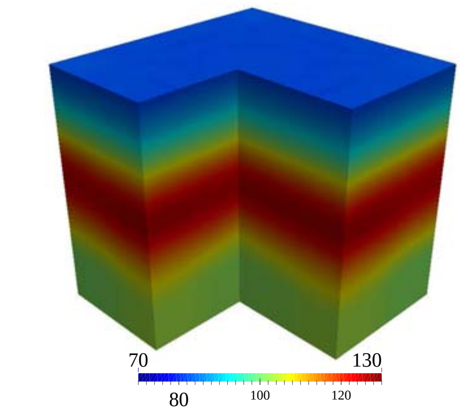

μ (inverted)

Single-parameter inversion (μ only)

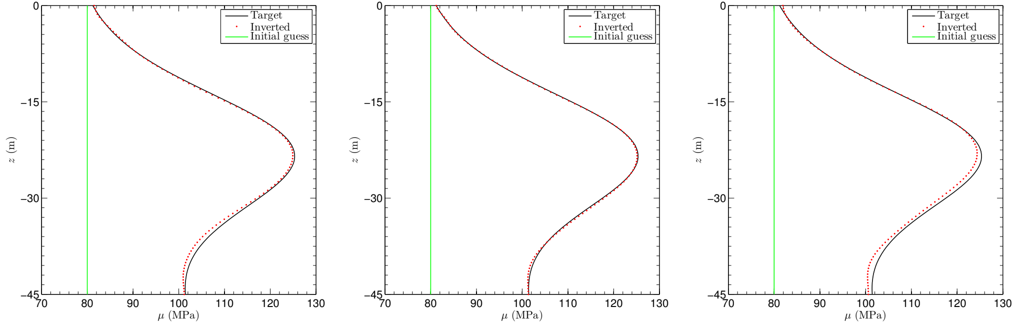

$(x, y) = (0, 0)$ $(x, y) = (10, 10)$ $(x, y) = (20, 20)$

Single-parameter inversion (λ only)

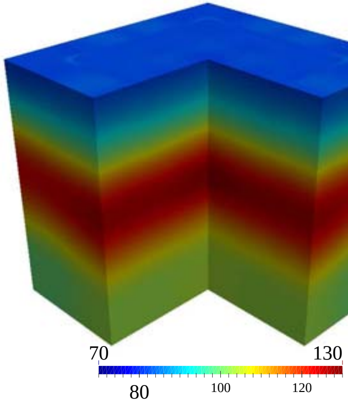

λ (inverted)

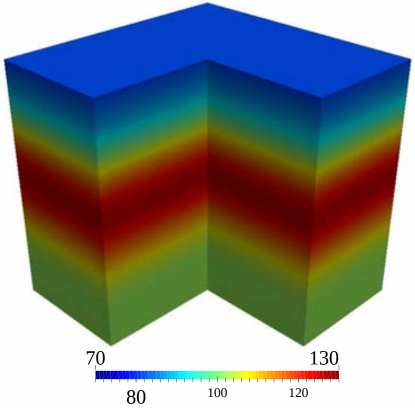

μ (a priori known)

Single-parameter inversion (λ only)

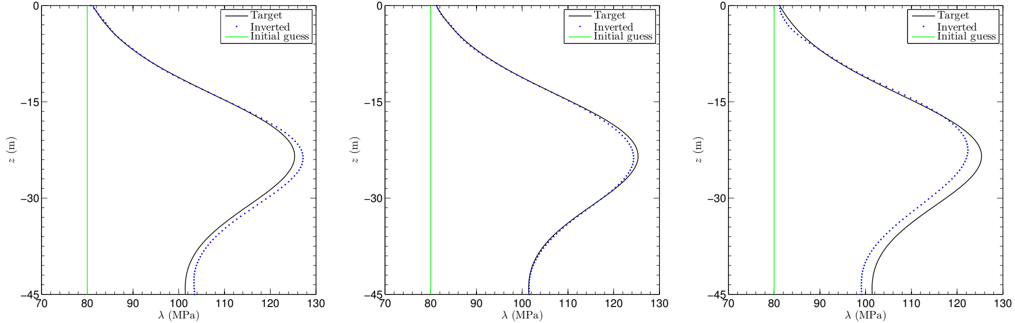

$(x, y) = (0, 0)$ $(x, y) = (10, 10)$ $(x, y) = (20, 20)$

Simultaneous inversion for λ and μ - unbiased

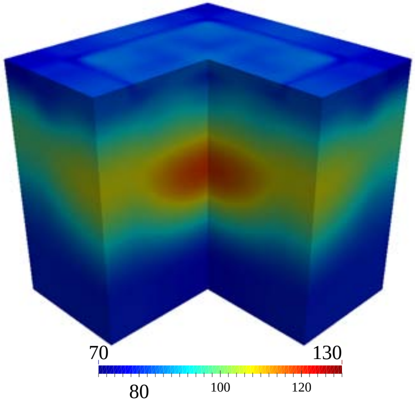

λ (inverted)

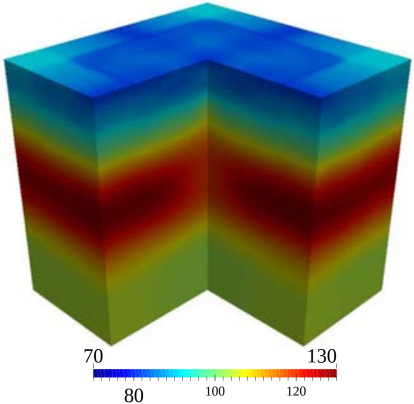

μ (inverted)

A physics-based algorithmic tweak

Bias search directions of λ by the search directions of μ during the early stages of the inversion process:

$$s_k^\lambda \leftarrow ||s_k^\lambda|| \left(W \frac{s_k^\mu}{||s_k^\mu||} + (1 - W) \frac{s_k^\lambda}{||s_k^\lambda||} \right)$$

$$W = 1 \rightarrow 0$$

Simultaneous inversion for λ and μ - biased

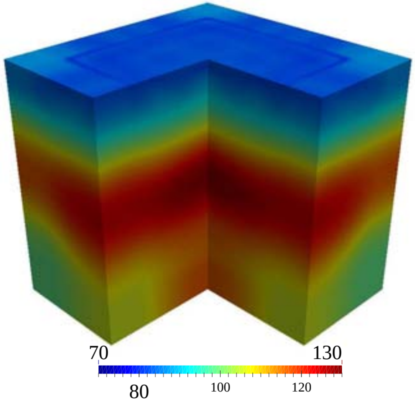

λ (inverted)

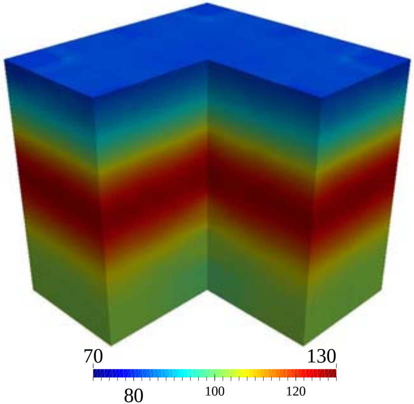

μ (inverted)

Simultaneous inversion: λ cross-sections

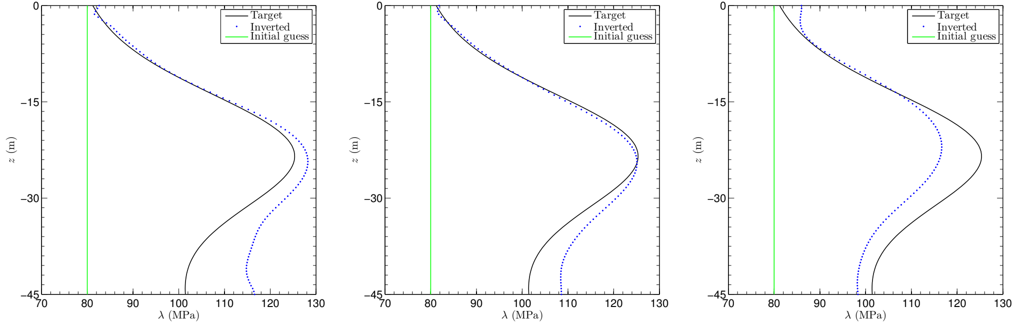

$(x, y) = (0, 0)$ $(x, y) = (10, 10)$ $(x, y) = (20, 20)$

Simultaneous inversion: μ cross-sections

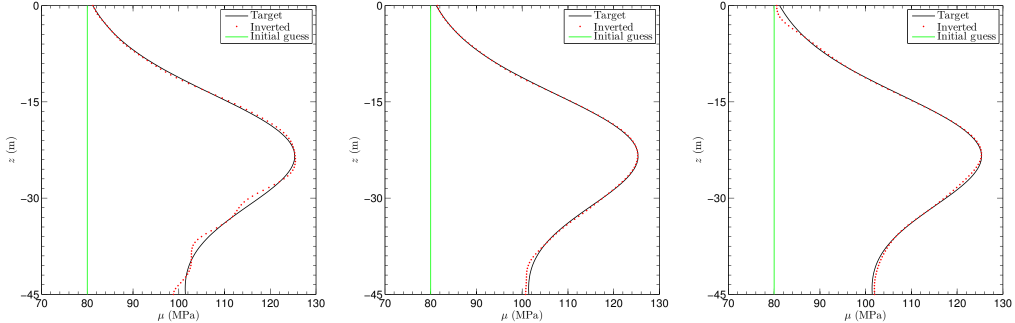

$(x, y) = (0, 0)$ $(x, y) = (10, 10)$ $(x, y) = (20, 20)$

Misfit history; frequency continuation scheme

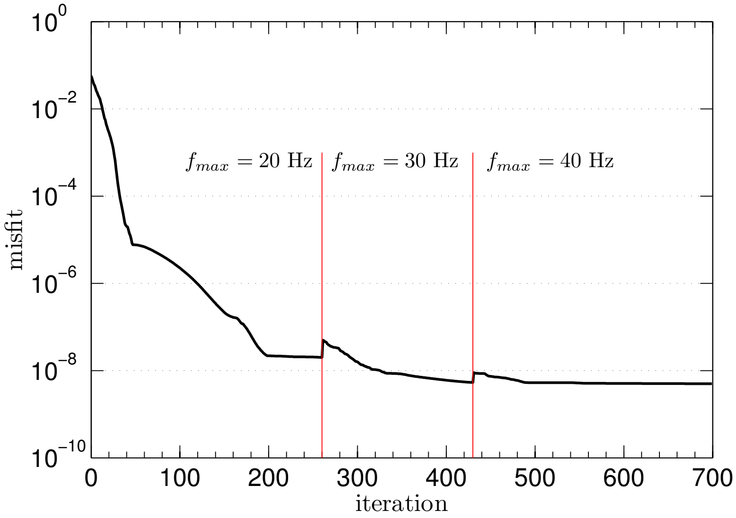

Example 2: setup

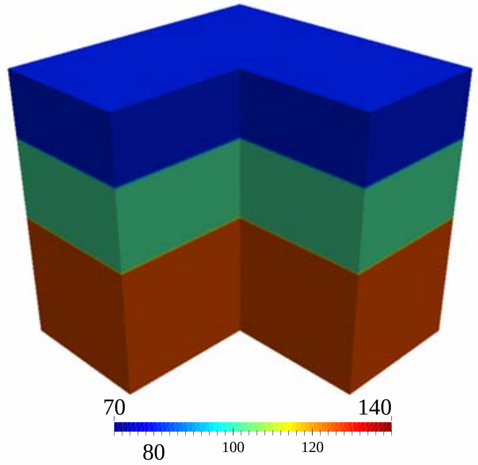

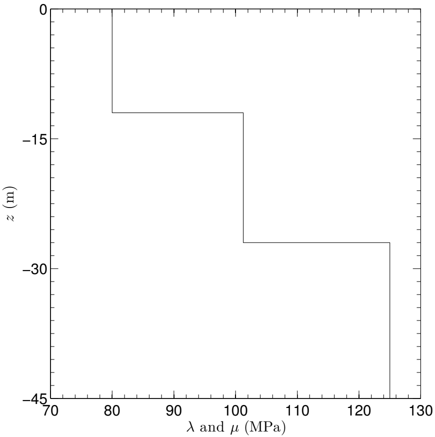

Layered medium: target λ and μ (MPa); and profile at $(x, y) = (0, 0)$

Simultaneous inversion ($f_{max} = 10$ Hz)

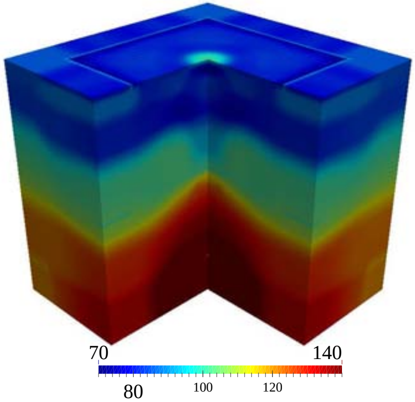

λ (inverted)

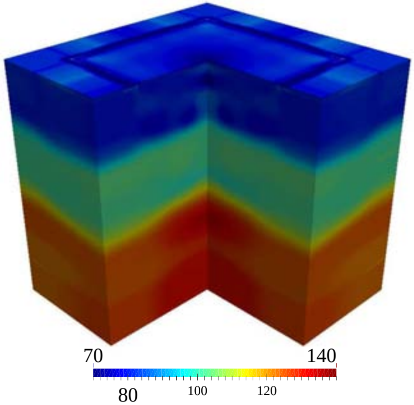

μ (inverted)

Simultaneous inversion ($f_{max} = 40$ Hz)

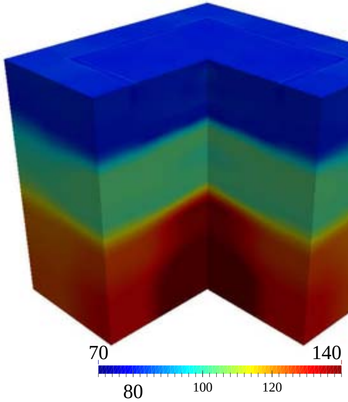

λ (inverted)

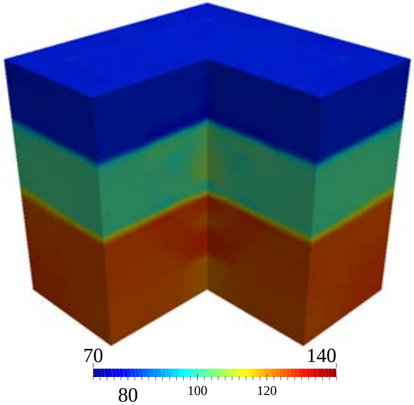

μ (inverted)

Example 3: setup

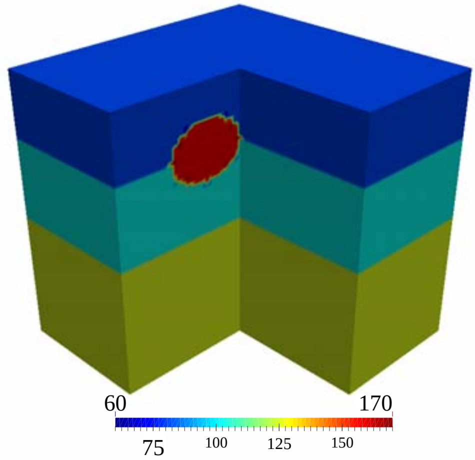

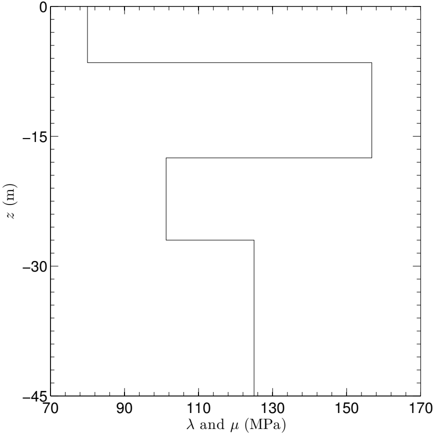

Layered medium: target λ and μ (MPa); and profile at $(x, y) = (7.5, 0)$

Simultaneous inversion ($f_{max} = 10$ Hz)

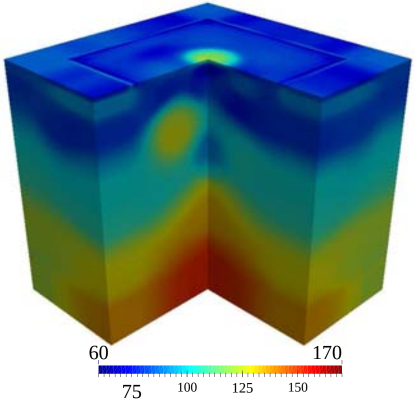

λ (inverted)

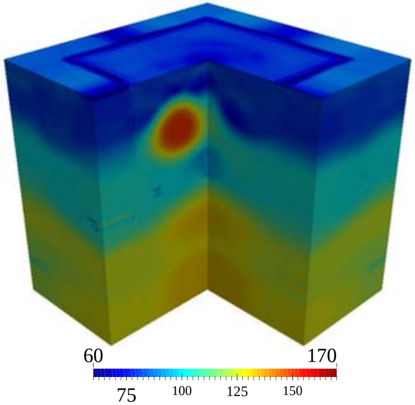

μ (inverted)

Simultaneous inversion ($f_{max} = 40$ Hz)

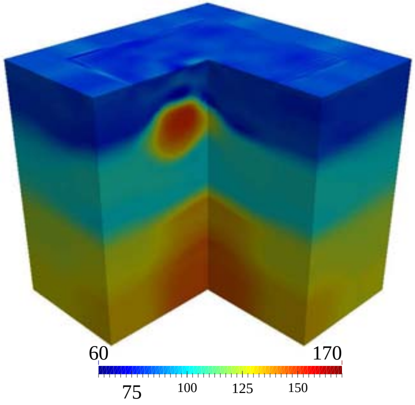

λ (inverted)

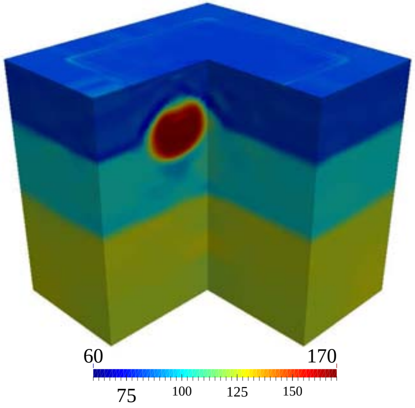

μ (inverted)

20% Gaussian noise, $f_{max} = 40$ Hz

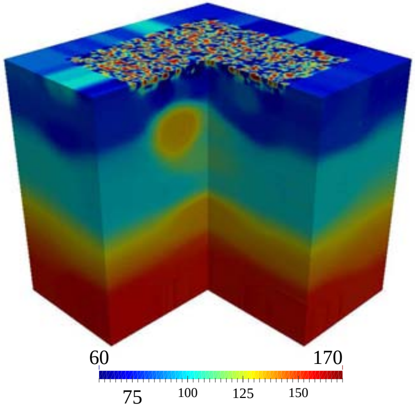

λ (inverted)

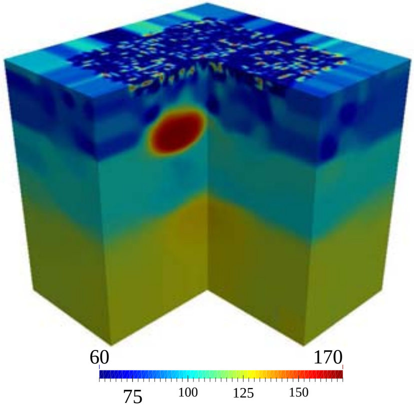

μ (inverted)

Inversion with Gaussian noise: λ, μ cross-sections

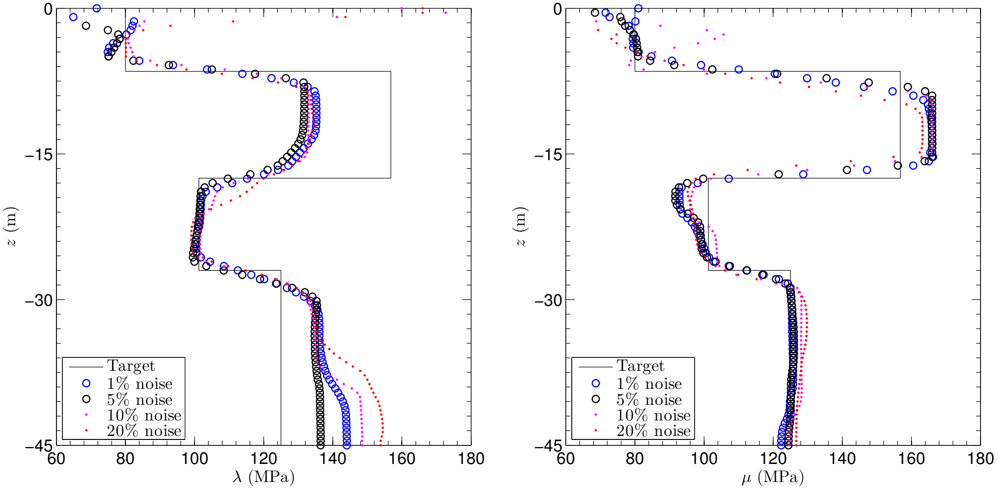

$$(x, y) = (7.5, 0)$$

Example 4: setup

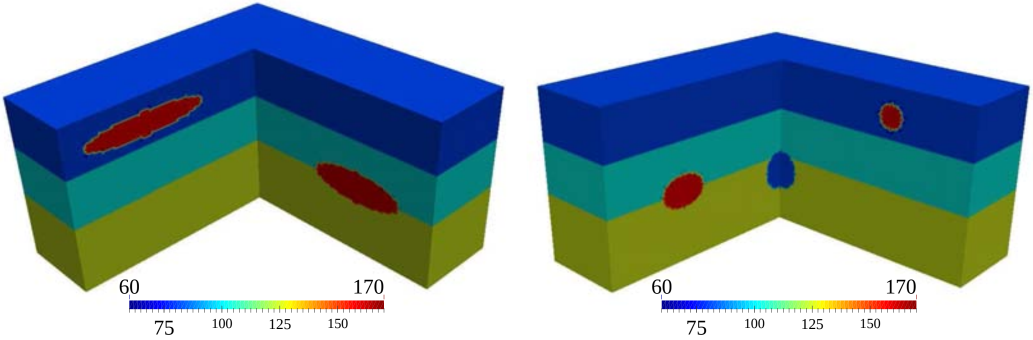

Layered medium with three inclusions: target λ and μ (MPa) at two different cross-sections.
state unknowns = 9,404,184; # material unknowns = 2,429,586
80 m $\times$ 80 m $\times$ 45 m medium

Example 4: setup

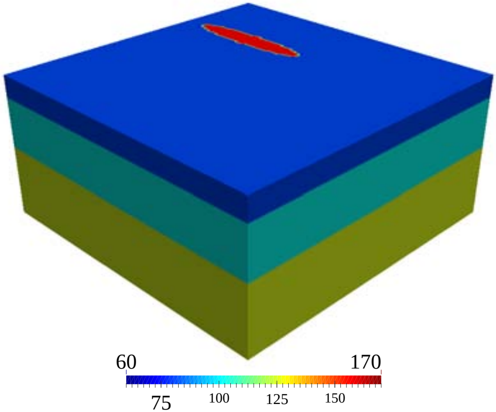

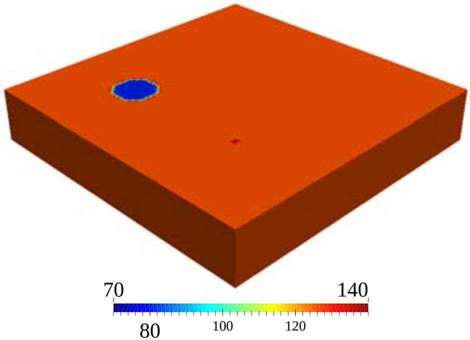

Layered medium with three inclusions: target λ and μ on
(left) the $z = -8.75$ m cross-section; and (right) the $z = -35$ m cross-section

Simultaneous inversion ($f_{max} = 40$ Hz)

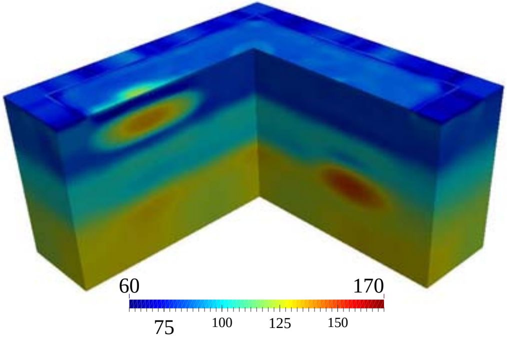

λ (inverted)

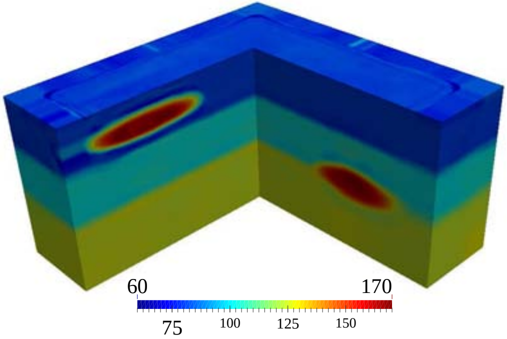

μ (inverted)

Simultaneous inversion ($f_{max} = 40$ Hz)

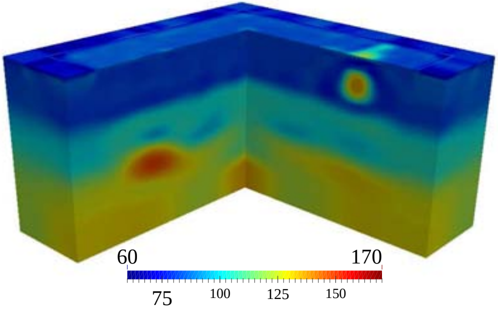

λ (inverted)

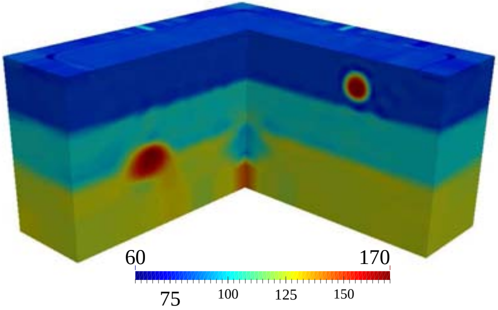

μ (inverted)

Simultaneous inversion ($f_{max} = 40$ Hz)

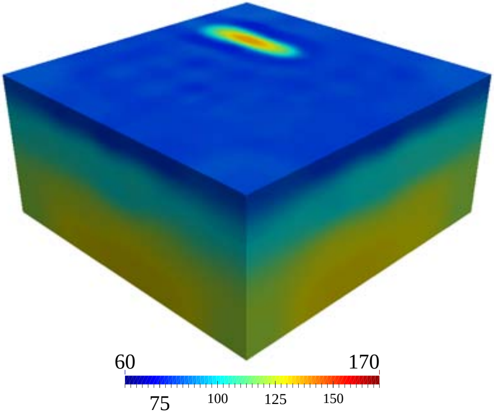

λ (inverted)

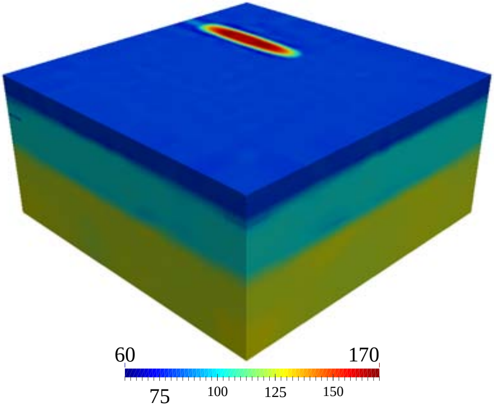

μ (inverted)

Simultaneous inversion ($f_{max} = 40$ Hz)

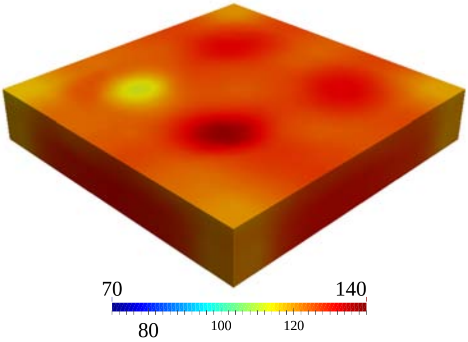

λ (inverted)

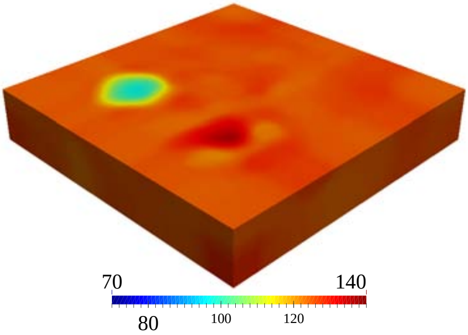

μ (inverted)

Outline

Garner Valley field experiment

The experiment layout

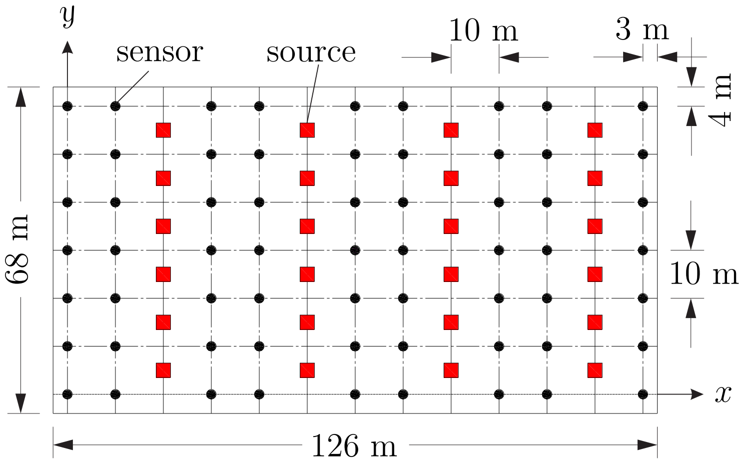

computational domain: 126 × 68 × 40 m + 10 m-thick PML
#material parameters: 718,566
#state unknowns: 3,885,648

FWI profiles

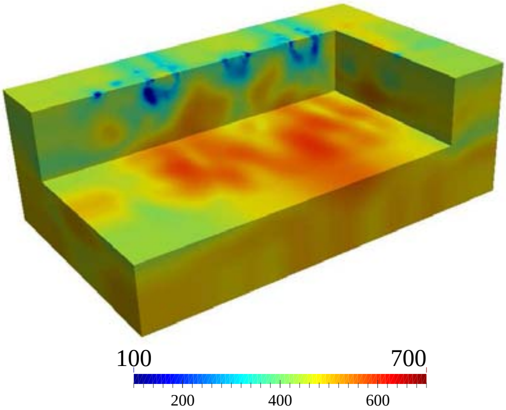

c_p (m/s)

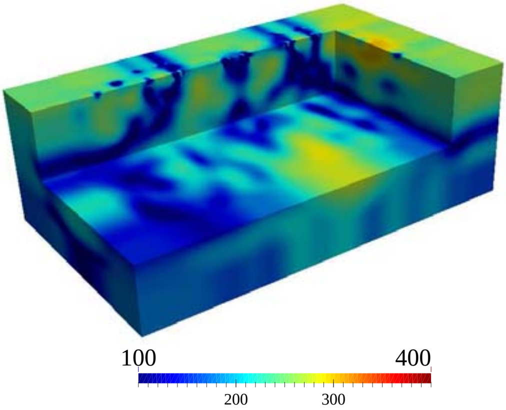

c_s (m/s)

SASW c_s profile

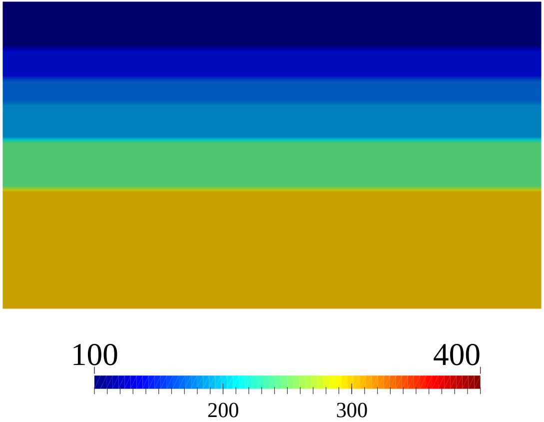

Cross-sectional profiles: $x = 10$ m

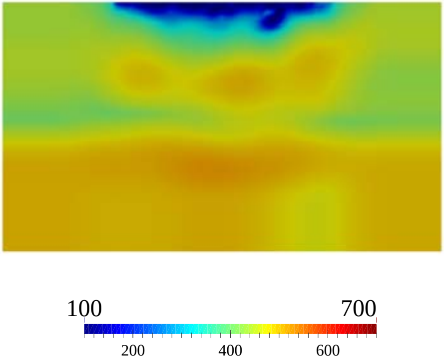

c_p (m/s)

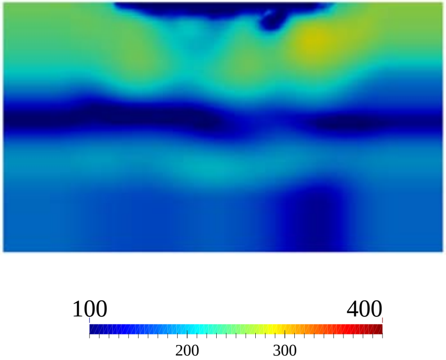

c_s (m/s)

Time-history comparisons: $x = +10$ m

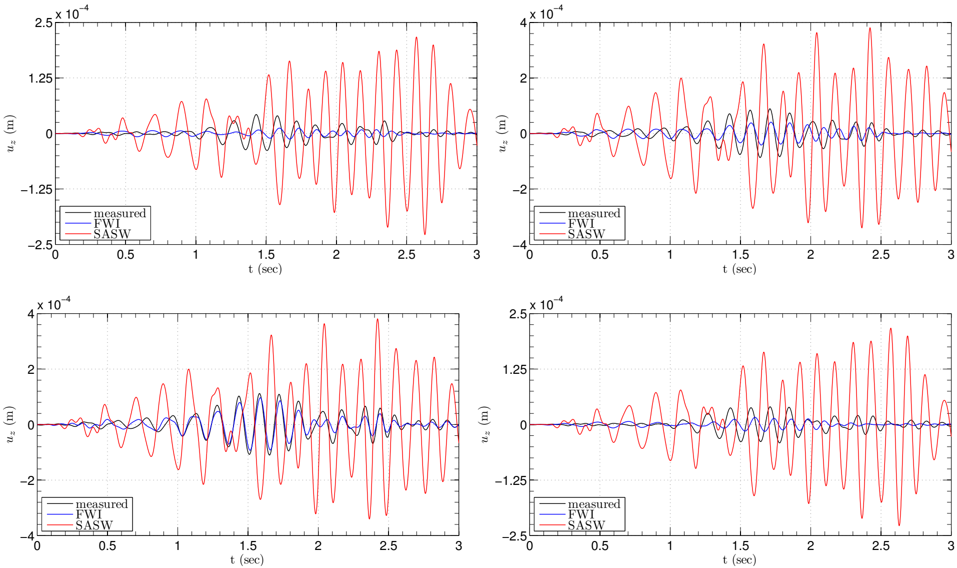

Sensor locations; from top-left to bottom-right: $y = 60, 40, 20, 0$ m

Time-history comparisons: $x = +90$ m

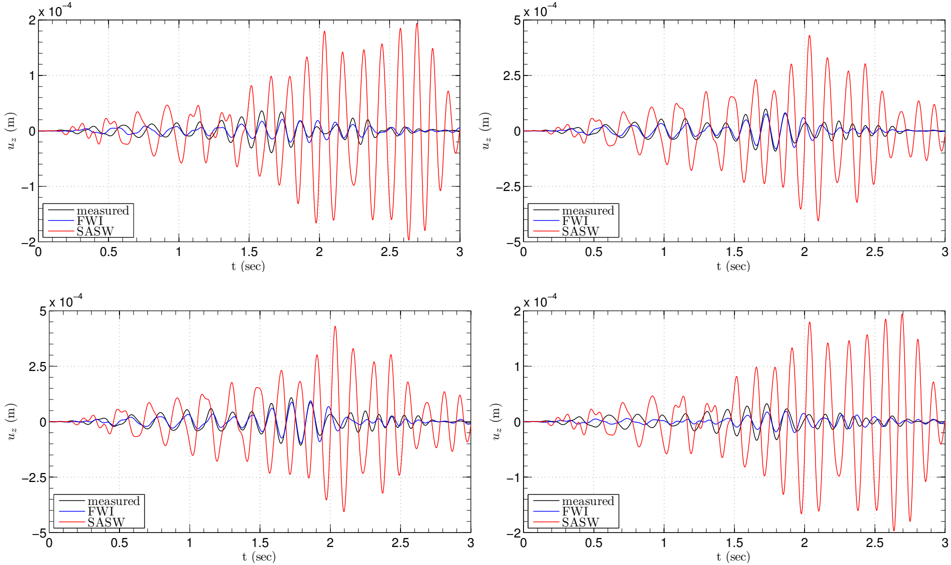

Sensor locations; from top-left to bottom-right: $y = 60, 40, 20, 0$ m

Time-history comparisons: $x = +100$ m

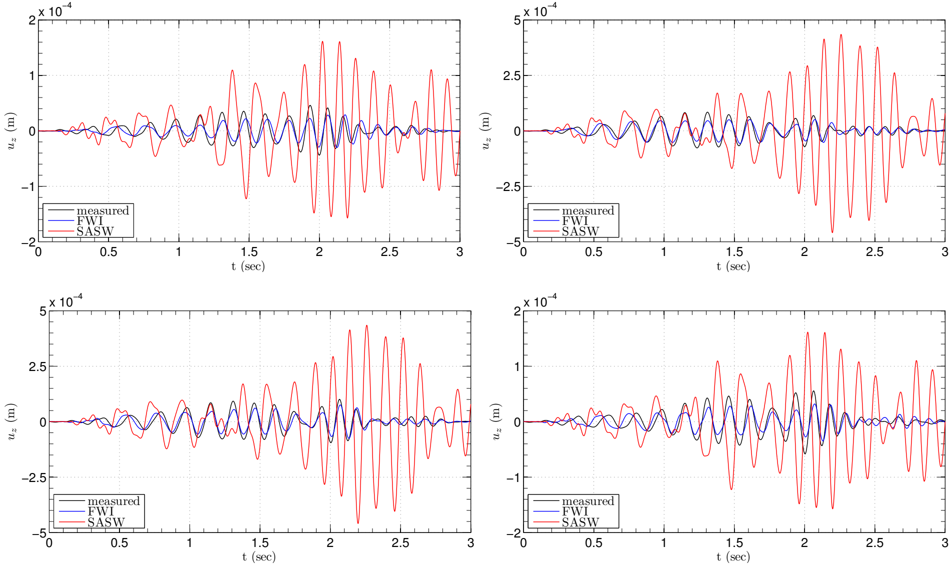

Sensor locations; from top-left to bottom-right: $y = 60, 40, 20, 0$ m

Outline

Summary

- A systematic framework for FWI-based site characterization

Outline

Challenges

- Material attenuation - inversion for attenuation parameters a huge challenge
- Real time - experiment steering
- Ground water level
- Beyond elasticity: poroelasticity / permeability
- Algorithmic improvements for speed and robustness
- Multi-physics probing (unlikely)
- Validation (difficult - control setting)

References

L. F. Kallivokas, A. Fathi, S. Kucukcoban, K. H. Stokoe II, J. Bielak, O. Ghattas
Site characterization using full waveform inversion, *Soil Dynamics and Earthquake Engineering, 47:62–82, 2013.*

A. Fathi, B. Poursartip, L. F. Kallivokas
Time-domain hybrid formulations for wave simulations in three-dimensional PML-truncated heterogeneous media, *International Journal for Numerical Methods in Engineering, 101(3):165-198, 2015.*

A. Fathi, L. F. Kallivokas, B. Poursartip
Full-waveform inversion in three-dimensional PML-truncated elastic media, *Computer Methods in Applied Mechanics and Engineering, in revision, 2015.*

A. Fathi, L. F. Kallivokas, K. H. Stokoe II, B. Poursartip
Three-dimensional site characterization using full-waveform inversion: theory, computations, and field experiments, *in preparation.*